JOURNAL OF MATERIALS SCIENCE **38** (2003) 901 – 907

A mechanistic analysis of the correlation between overall strength and indentation hardness in discontinuously reinforced aluminum

B. D. KOZOLA, Y.-L. SHEN*
Department of Mechanical Engineering, University of New Mexico, Albuquerque, NM 87131
E-mail: shenyl@me.unm.edu

It is well established that the indentation hardness of metallic alloys shows a reasonable correlation with their yield strength or ultimate strength. Experiments illustrate that such a unique correlation is nonexistent for discontinuously reinforced metal matrix composites, even when the indentation size is much greater than the reinforcement size. For aluminum alloys reinforced with silicon carbide particles, the same composite yield strength and tensile strength with different reinforcement fractions do not lead to similar hardness, or vice versa. Finite element analyses are carried out to rationalize the experimental findings. The modeling utilizes a two-dimensional plane-strain formulation. Discrete particles are included in the material model, and the overall stress-strain response and the indentation response are numerically simulated. The results confirm the lack of unique correspondence between the composite hardness and strength. The alteration of local heterogeneity in the composite is found to affect the indentation response. Effects of the geometrical arrangement of particles and thermal residual stresses on the indentation response are also investigated numerically.

1. Introduction

Hardness tests are routinely used as a simple and effective means of quantifying the mechanical strength of materials. Although the indentation hardness in itself is not a well-defined material parameter, the correlation between various hardness scales and tensile strength has been compiled for a variety of metals and alloys [1]. When a metal is discontinuously reinforced with ceramic particles to form a metal matrix composite, higher stiffness, higher ultimate strength and lower ductility can be observed. The composite displays a stronger strain hardening behavior in the tensile and compressive tests. The overall elastic-plastic nature of the composite, however, possesses a qualitative resemblance to that of the unreinforced metals (see, e.g., references [2–4] for review). This may imply that the composite, viewed as a continuum, is amenable to traditional hardness tests for characterizing its mechanical properties, since we concern here only the cases when the size of the indenter is much greater than the size and interspacing of particles in the composite.

As metal matrix composites are generating increased interest for industrial applications, the need for understanding the relationship between hardness and overall strength has been recognized [5–9]. Careful analyses of experimental data showed that the use of hardness to predict the tensile flow stress of particle reinforced aluminum (Al) matrix composites is prone to overestimates [6–9]. This is partially due to internal damage in the form of particle cracking, which weakens the material in the uniaxial tensile response but not in the hardness response [6, 8]. However, in the case of composites with small reinforcement particles where particle cracking is largely not of concern, a correlation between hardness and overall strength is still not found [7, 8]. The hardness test consistently overestimates the yield strength and ultimate tensile strength of the composites. This is especially true in cases where the strength of the Al matrix is relatively low.

In the present work, we seek to provide a mechanistic rationale for the experimental findings. Computational modeling of uniaxial tensile/compressive loading and indentation loading was carried out. The finite element analysis takes into consideration the discrete particles in the composite system. In the following sections experimental results are first summarized. The computational approach and results are then presented. The correspondence between modeling and measurement, as well as issues regarding indentation modeling of heterogeneous materials in general, are also discussed.

2. Experiments

The 2080 Al alloy (Al-3.6Cu-1.9Mg-0.25Zr), unreinforced and reinforced with 10 and 20 vol.% silicon carbide (SiC) particles, were used in this study. All

*Author to whom all correspondence should be addressed.

materials were processed by the powder metallurgy route and extruded. The average reinforcement particle size after extrusion is about 6 μm. Due to the relatively small SiC particle size the fraction of fractured particles after extrusion is insignificant. A T8 thermomechanical treatment [10] was applied to the composites and the unreinforced alloy. The materials were solution treated at 493°C, quenched in water, cold rolled to 5% reduction in thickness, and aged at 175°C for 24 h (to the peakaged condition). The rolling step provides a homogeneous distribution of dislocations that serve as sites for heterogeneous nucleation of precipitates. As a consequence, preferential precipitation in the matrix immediately adjacent to the particles due to processing induced thermal stresses can be avoided, which was microscopically confirmed [11]. The nearly identical microstructures in the composite and the monolithic alloy make possible a valid comparison of material properties in the present study. Some peakaged materials were heat-treated further to the overaged condition for 24 h each at 200, 225 and 250°C.

Tensile tests were conducted on a servohydraulic load frame at a strain rate of 10^{-3} s^{-1}. The yield strength and ultimate strength values reported in this paper were those averaged over three sets of tests. The standard Rockwell B-scale test, featuring a 1.588 mm-diameter spherical steel indenter, was used to characterize the hardness [12]. The Rockwell B-scale hardness test is commonly applied to quantifying the mechanical strength of a wide variety of Al alloys. A minor load and a major load of 10 kg and 100 kg, respectively, were imposed on the specimen. The hardness value (HRB) is directly determined by the depth of indentation beyond the minor load. The hardness values reported in this paper were those averaged over at least five readings; different readings obtained from the same material had a scatter range of less than 3 HRB. Fig. 1 shows a representative micrograph of the hardness tested composite containing 20% SiC particles near the indentation site. More details of the experimental procedure can be found in reference [8].

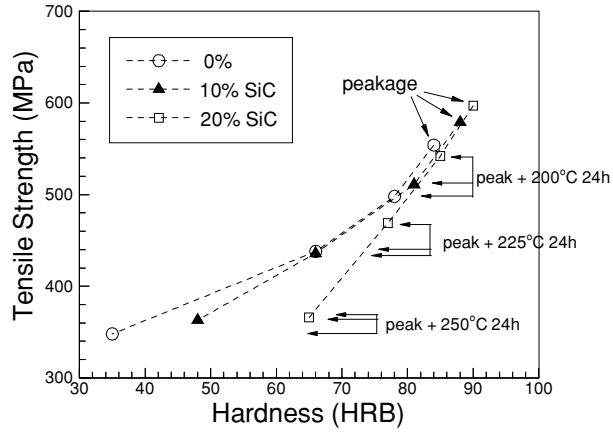

Figure 2 Relationship between true ultimate tensile strength and Rockwell B-scale hardness of the composites and unreinforced alloy obtained from experiments. Data from the peakaged and three overaged states are indicated.

Fig. 2 shows the true ultimate tensile strength as a function of hardness (HRB) for the composites (with 10% and 20% reinforcement concentration) and the monolithic (0%) alloy. The points in the upper-right end of the three curves correspond to the peakaged materials, showing the increase in tensile strength and hardness with increasing reinforcement volume fraction. The tensile strength and hardness of the materials decrease significantly with the severity of overaging treatment. A very notable feature, however, is that the data in Fig. 2 do no follow a simple relation as with typical metallic materials. With decreasing matrix strength (increasing overaging) the difference in tensile strength of the three materials is reduced, but the disparity in hardness increases significantly. In the overaged condition, the composite with a higher reinforcement fraction shows a much greater hardness value, although its tensile strength is comparable to those with lower particle

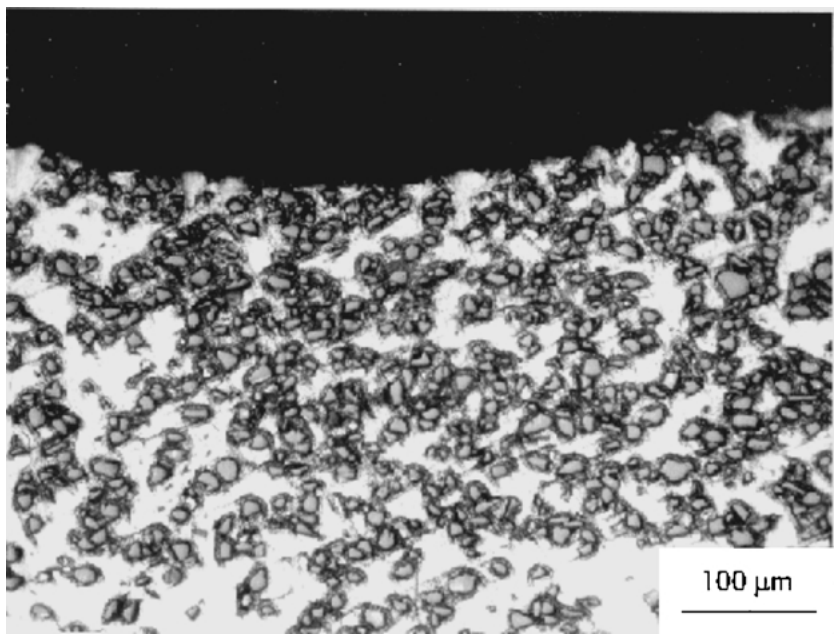

Figure 1 Optical micrograph of the composite containing 20% SiC particles, taken near the indentation site.

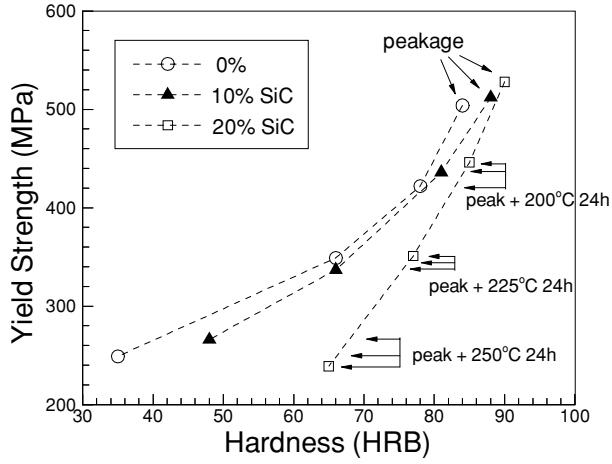

Figure 3 Relationship between true 0.2% offset yield strength and Rockwell B-scale hardness of the composites and unreinforced alloy obtained from experiments. Data from the peakaged and three overaged states are indicated.

fractions. Equivalently speaking, when the strength of the Al matrix is relatively low, a wide range of hardness is found even when all materials exhibited similar tensile strength. The hardness of the overaged composite appears to be dominated by the volume fraction of reinforcement.

The results shown in Fig. 2 may be potentially influenced by microscopic damage such as particle cracking, which can occur when the composite is loaded to close to its ultimate tensile strength. Tensile loading induced damage is of much less concern if one compares the yield strength, rather than tensile strength, with hardness. Fig. 3 shows the true yield strength (0.2% offset) as a function of hardness for all the materials and aging treatments included in Fig. 2. The trends for yield strength and tensile strength are similar. Again, the data do not follow a simple relation, which suggests that the lack of unique correspondence between overall strength and indentation hardness is an intrinsic behavior of the composite.

It is noted that the hardness disparity caused by overaging observed in Figs 2 and 3 is not due to the higher elastic modulus of the composite with increasing reinforcement concentration, because aging treatment does not alter the elastic properties of Al matrix in the respective composites. In attempting to rationalize the experimental results, numerical modeling was performed as presented in the following sections.

3. Numerical modeling

3.1. Model

Two dimensional finite element analyses were carried out to simulate the tension, compression and indentation loading conditions. A square computational domain (implicitly taken as 1 mm $\times$ 1 mm in size) containing spherical particles embedded within the matrix is used. A representative finite element mesh with a regular square alignment of particles is shown in Fig. 4. Four noded bilinear elements were used. The SiC particles are assumed to be linearly elastic, with Young's modulus 450 GPa and Poisson's ratio 0.17. The Al matrix is taken to be elastic-plastic, with Young's modulus 72 GPa and Poisson's ratio 0.33. The plastic response of matrix follows rate-independent von Mises plasticity with isotropic hardening. There is a linear hardening regime between the initial yield strength (σ_0) and the maximum strength (σ_u) taken at a plastic strain of 0.10;

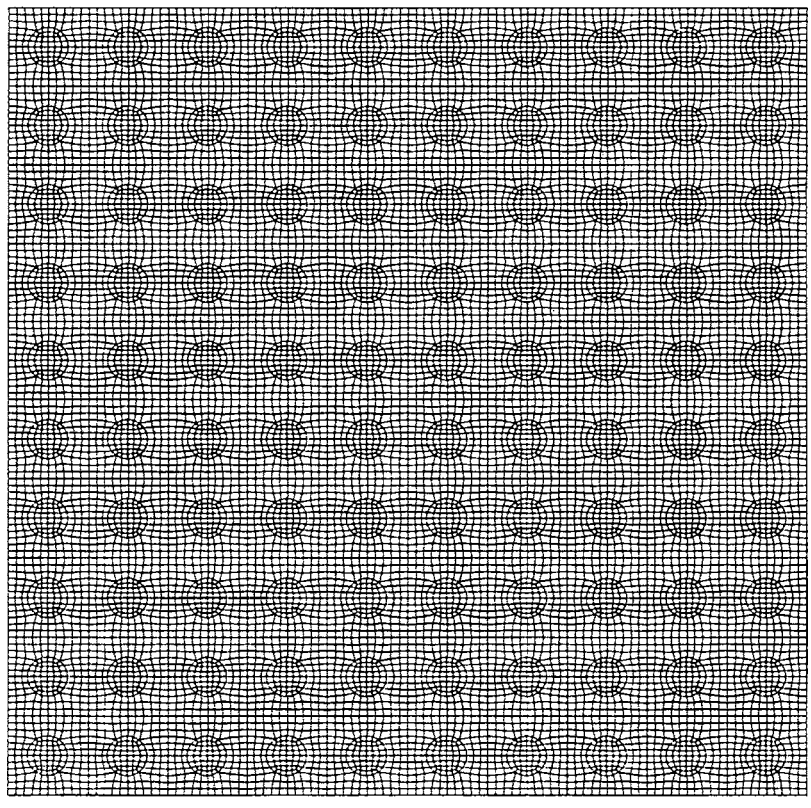

Figure 4 A representative finite element mesh having a total of 100 regularly arrayed circular particles.

beyond σ_u a perfectly plastic response ensues. Three different plastic properties are used in the current study: (i) $\sigma_0 = 400$ MPa and $\sigma_u = 600$ MPa, (ii) $\sigma_0 = 300$ MPa and $\sigma_u = 500$ MPa, and (iii) $\sigma_0 = 200$ MPa and $\sigma_u = 400$ MPa; they were devised to simulate the matrix material with increasing extent of overaging. Although overaging generally results in decreasing ductility, a fixed plastic strain value where σ_u is attained was still assumed in all three cases. This is deemed appropriate due to the facts that the modeling result is dominated by the significantly different σ_u values and that our T8 treated materials showed very small strain hardening beyond the beginning stages of plastic yielding [6, 8] so the variation of strain at σ_u has a very small influence in the numerical result. The model composites based on these three matrix properties are henceforth referred to as "high strength, "medium strength" and "low strength" materials, respectively.

In all calculations the thermal residual stresses are included. Thermal residual stresses, generated from cooling during processing, inevitably exist in metal matrix composites due to the mismatch in coefficient of thermal expansion between the ceramic reinforcement and metal matrix. In the present study we incorporate a cooling step by imposing a spatially uniform temperature change from 500°C (presumably the stress-free temperature where the Al matrix undergoes solution treatment) to 20°C, prior to all forms of mechanical loading. The coefficients of thermal expansion used for the SiC reinforcement and the Al matrix are, respectively, 4.5×10^{-6} K^{-1} and 22.0×10^{-6} K^{-1}. In the modeling of thermal cooling, the elastic, plastic and thermal properties are those specified above and assumed to be rate independent and temperature independent for simplicity.

The plane-strain formulation is employed. The plane strain approach is able to capture the qualitative features of composite response and internal field evolution in the actual three-dimensional layout [13–15]. Uniaxial loading is simulated by prescribing relative displacements on the top and bottom boundaries. Effectively this was achieved by employing the commonly adopted unit-cell model involving only one particle and appropriate boundary conditions [13, 14] for composites with regularly aligned particles (Fig. 4). At any specified strain the composite flow stress can be directly obtained from modeling and later used for correlating with the indentation response. Within the context of the present approach, the composite tensile and compressive stress-strain curves are largely equivalent [14, 16]. Therefore, the results presented here are considered valid for both situations.

Hardness indentation is simulated by pressing a rigid circular indenter into the top face. Because of symmetry the computational domain in Fig. 4 is treated as one half of the structure with its left-hand boundary being the axis of symmetry (see also Fig. 7 below). The ratio of the indenter radius and the initial side length of the specimen is taken to be 0.79. During indentation the bottom boundary is allowed to slip tangentially. The top boundary is not constrained except that when a contact with the rigid indenter is established, a coefficient of friction of 1.0 is imposed. The right-hand boundary is free to move but was constrained to remain vertical. Setting the right-hand boundary entirely free produces only a slightly different indentation response [16]. Further details of the indentation modeling are discussed in Section 4.

The finite element code ABAQUS [17] was used for the modeling with large deformation accounted for in all cases. We consider four reinforcement area fractions: 0%, 10%, 20% and 30%, each with three different matrix properties as introduced above. To compare the indentation response, a hardness measure within the present modeling framework needs to be defined. We use the formula $H = 130–3{,}000d$, which is similar to that used in determining the Rockwell hardness, with H being the presently defined "hardness number" and d the penetration depth in mm. The hardness number is calculated with an arbitrarily chosen constant load of 125 N. The combination of this load and the formula chosen is such that the hardness numbers obtained from our modeling are within the range from about 30 to 100, which roughly corresponds to the valid HRB values in reality. Note that our two-dimensional analysis does not conform to the experimental requirement for the Rockwell hardness test (or any other standard test). Nevertheless, the objective here is simply to define a reasonable numerical hardness measure to facilitate a direct but qualitative comparison with the experimental results. When presenting the comparison of overall composite response with hardness, two levels of composite flow stresses, taken directly from the calculated stress-strain curves, are used: the offset yield stress at 0.002 plastic strain and the stress at 0.10 total strain.

3.2. Results

Before the correlation between composite strength and hardness is presented, we first show representative results of uniaxial stress-strain response and indentation response. Fig. 5 shows the modeled tensile true stress-true strain curves of the composites with a reinforcement area fraction of 20%. The three different matrix

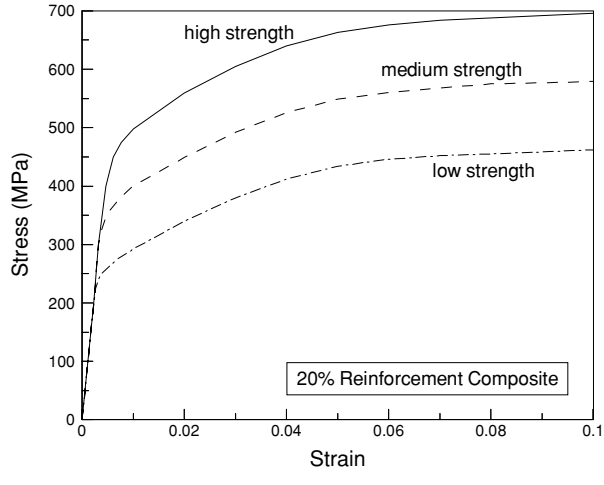

Figure 5 Calculated tensile true stress-true strain curves of the composites with reinforcement area fraction of 20%. Results from the three different matrix plastic properties are included.

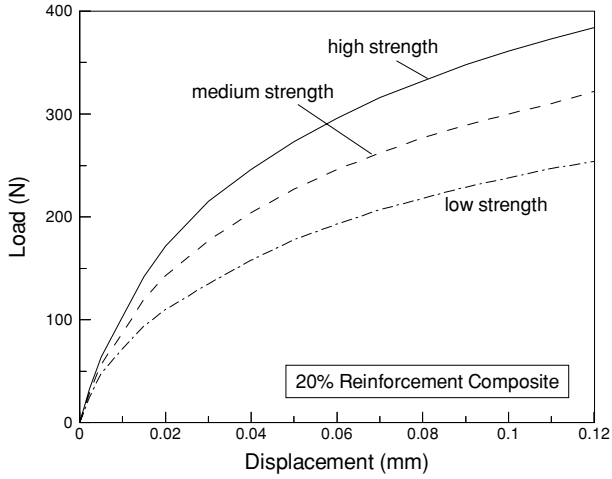

Figure 6 Calculated indentation response of the composites with a reinforcement area fraction of 20%. Results from the three different matrix plastic properties are included.

strengths give rise to distinctly different composite response, as expected. Although within the strain range considered in Fig. 5 the matrix material is treated as elastic-plastic with linear hardening, the incorporation of reinforcement leads to non-uniform local deformation in the matrix [4, 14] so a smooth stress-strain response is obtained. The composites with other reinforcement concentrations show the same trend.

Fig. 6 shows the modeled indentation response of the composites with a reinforcement area fraction of 20%, in the form of load vs. displacement (penetration depth). It is evident that a stronger matrix results in a harder indentation response. The composites with other reinforcement concentrations show the same trend. Fig. 7 shows the contours of constant equivalent plastic strain for the 20% reinforcement composite with the "high strength" matrix at an indentation displacement of 0.05 mm. The particles in the left part of the specimen are well discerned because no plasticity exists in the purely elastic particles. The presence of discrete particles dramatically fragments the plastic strain field and forces the plastic flow into a banded structure. The large degree of plasticity, however, decays quickly with increasing distance from the indentation site. A notable feature in Fig. 7 is that the particles directly underneath the indentation are displaced downward with the surrounding matrix, with the interparticle spacing along the vertical direction reduced compared to other regions. Effectively this represents a local increase in particle concentration. The local increase in particle concentration "felt" by the indenter, accompanied by the severe work hardening of the mechanically constrained matrix, can lead to an artifact that the composite becomes increasingly harder (locally) as the indentation progresses.

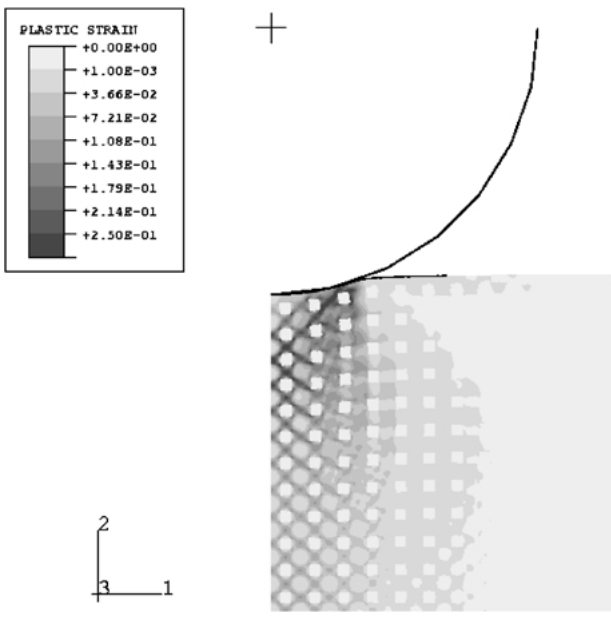

Figure 7 Contours of constant equivalent plastic strain developed during indentation modeling when the indentation displacement is 0.05 mm.

Figs 8 and 9 show the relationship of modeled tensile flow stress and modeled hardness number for all the composites considered in this study. The two figures are presented in the same form as the experimental results (Figs 2 and 3) for the purpose of a qualitative but direct comparison. For the overall composite strength, a lower stress level (0.002 offset yield, Fig. 8) and a higher stress level (at 0.10 total strain, Fig. 9) were chosen to

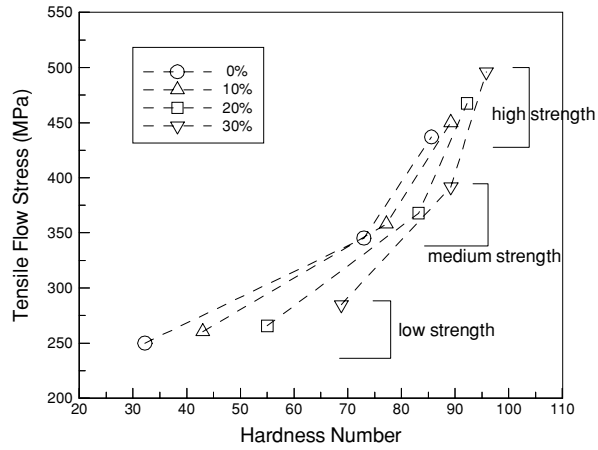

Figure 8 Relationship between the modeled tensile flow stress and modeled hardness number of the composites. The tensile flow stress is chosen as the 0.002 offset yield stress. The hardness number is defined in Section 3.1.

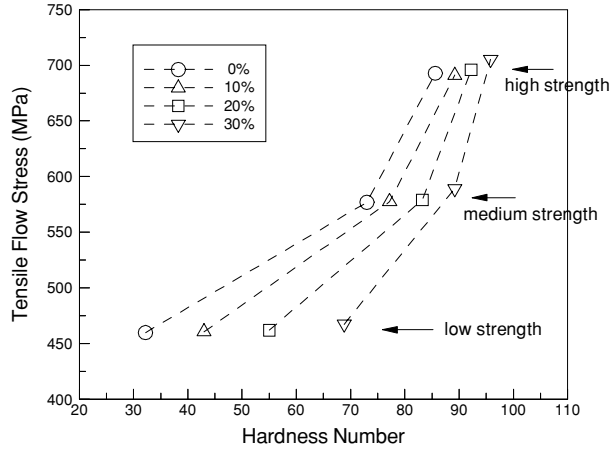

Figure 9 Relationship between the modeled tensile flow stress and modeled hardness number of the composites. The tensile flow stress is chosen as the stress at 0.10 total strain. The hardness number is defined in Section 3.1.

illustrate the generality of the numerical results. It can be seen that both figures show the same trend. At low composite strength a large disparity in hardness exists for composites with different reinforcement concentrations; at high composite strength the hardness numbers tend to converge, meaning that the hard reinforcement plays a less important role when the matrix material becomes stronger. The numerical results are in agreement with experimental findings.

4. Discussion

4.1. Modeling vs. experiments

The lack of unique correspondence between hardness and overall strength of the composite is due to the fundamental difference in deformation caused by the two modes of loading. During a tensile or compressive test, the material within the gage section undergoes nominally uniform deformation. In a hardness test, however, severe plastic flow is concentrated in the localized region directly below the indentation, outside of which the material still behaves elastically [18]. This is also illustrated from the present numerical modeling. Although plastic deformation itself is not responsible for volume change, the superposition of very large hydrostatic pressure under the indentation (well exceeding 1 GPa locally in the matrix according to the present modeling) can contribute to a greater volumetric contraction of the metal matrix compared to the ceramic particles. For instance, for the 20% reinforcement composite with the "high strength" matrix, the concentration of particles increases to about 22.2% at a distance of two inter-particle spacing directly below the indentation when the indentation depth is 0.05 mm. As the indenter moves downward during the test, the pressure is accommodated by the severely constrained matrix flow along with the localized increase of particle concentration, which tends to increase the resistance to deformation. Consequently, if there is an intrinsic correlation between hardness and mechanical strength for the metal matrix, then, for the composite, the hardness reading will tend to overestimate the measured overall strength. With a decreasing matrix strength the effect of reinforcement becomes increasingly prominent (Figs 2, 3, 8 and 9).

A legitimate concern at this junction is if the present two dimensional analysis is capable of capture the three dimensional effects occurred in actual materials. Since it will be extremely computationally demanding to incorporate discrete particles in a three dimensional model and still obtain mesh independent results, the *plane strain* condition is adopted here. In a previous attempt an indirect approach involving a *plane stress* analysis was undertaken [8, 19]. The overall stress-strain response of a particle-matrix system was first obtained from finite element modeling. The stress-strain response then served as the inherent properties of a homogeneous material subject to indentation modeling. In a parallel fashion, indentation modeling was directly conducted on the two-phase composite system. To avoid the complexities caused by plane strain when carrying the simulated overall stress-strain response to the homogenized material model due to the constraint in the third direction, the plane stress condition was enforced in all calculations there. Although the two-phase system and the homogenized system possessed exactly the same overall stress-strain behavior, the two-phase model consistently showed a significantly harder response than the homogenized model under indentation. The numerical finding, in agreement with the experiments in essence, can also be explained by the local increase in particle concentration discussed above. The fact that both the indirect plane stress approach and the direct plane strain simulation result in qualitatively the same conclusions is a strong indication of the validity of the current analysis.

4.2. Other modeling issues

Several factors which have not been addressed thus far can potentially influence the indentation modeling results: the number of particles included in the numerical model, the geometrical arrangement of particles, and the effect of thermal residual stresses existent in actual composites. Attention is devoted to these effects in this section.

A simple question to ask is: were enough particles included in the model so the indent size can indeed be considered much greater than the particle size? To answer this one can examine the convergence of numerical results by varying the total number of particles under a fixed particle concentration. Fig. 10 shows such a comparison of load-displacement response during indentation, with the area fraction of particles being 0.20 in all cases and the number of particles included in the model being increased from one to 144. The "high strength" matrix is used is this case. All particles are regularly aligned, with the one-particle case having a single large particle at the center of the square computational domain. The one-particle case has a softer response owing to the fact that the matrix makes the most contribution in resisting the indentation, especially at the early stages. As the number of particles increases, the indentation response soon converges. The curves for the cases of 100 and 144 particles show essentially

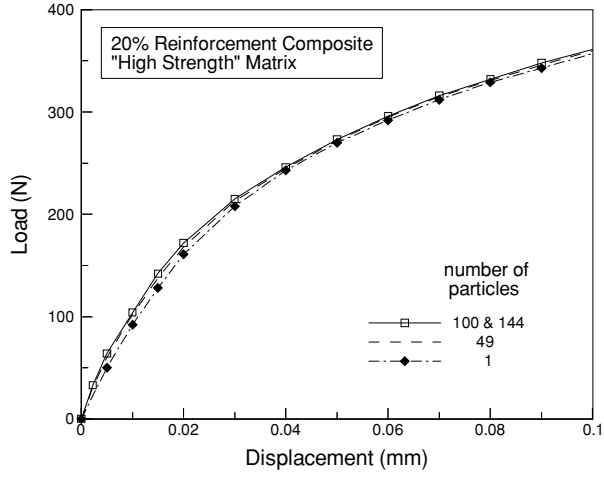

Figure 10 Calculated load-displacement response during indentation for different total numbers of particles included in the model. The area fraction of particles is fixed at 0.20.

no difference. As a consequence, it is reasonable to conclude that the present numerical study is representative of the "many particles" scenario.

The effect of reinforcement arrangement is investigated through several composite models containing particles that have different spatial distributions. These include two types of regular but staggered (rather than square-packed as in Fig. 4) arrangements and four types of random arrangements, all with a total of 100 particles at a fixed particle area fraction of 0.20 [16]. The indentation load-displacement curves all displayed very little difference from those of regular square arrangement (Fig. 6), except for very slight fluctuations from case to case. Therefore, the effect of particle arrangement on the indentation response is insignificant.

Lastly, there is a need to examine the effect of thermal residual stresses on the indentation response. Previous numerical modeling with thermal stresses accounted for showed that, for discontinuously reinforced metals with a matrix capable of strain hardening, the apparent modulus and initial yield strength of the composite are lowered but after a certain degree of yielding the flow stress is elevated, compared to the case without any thermal history [14]. Although all the numerical results presented in this paper so far have the built-in thermal history, we have also carried out modeling where the thermal cooling step is ignored for the purpose of studying the effect of thermal residual stresses on a theoretical basis. Fig. 11 shows a representative comparison of the indentation load-displacement response. Here the composite has 100 regular square-arrayed particles and the matrix is of "high strength." It can be seen that the difference for the two cases is small. At the early stages of indentation the presence of thermal residual stresses renders a slightly softer response, but the two curves soon approach one another at greater displacements. It can be concluded that the effect of thermal residual stresses on the indentation response is small. In actuality, if thermal residual stresses are not accounted for in all the calculations in this study, the hardness-strength relationship shown in Figs 8 and 9 will only be affected slightly with the trends remaining the unaltered.

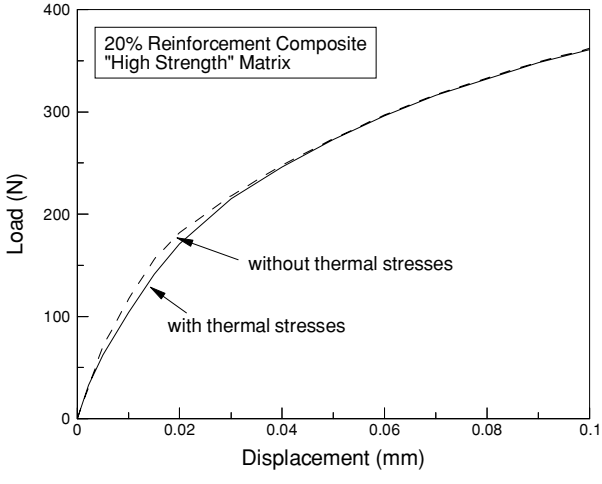

Figure 11 Calculated load-displacement response during indentation with and without a prior cooling step. The composite has 100 regular square-arranged particles with an area fraction of 0.20.

5. Conclusions

Experimental measurements of 2080 Al alloy discontinuously reinforced with SiC particles showed that indentation hardness does not scale with the overall composite strength, even when the indentation size is much greater than the reinforcement size. This is contrary to that found in most monolithic metals and alloys. Hardness testing tends to overestimate the composite tensile/yield strength, especially in cases where the matrix strength is relatively low. Finite element modeling, featuring discrete particles embedded within the metal matrix, of the composite stress-strain response and indentation hardness was performed. The numerical analysis showed the same trend as the experiment, rationalizing the lack of unique relationship between hardness and composite strength. It is illustrated that the higher hardness is associated with the localized increase in particle concentration directly underneath the indented region where severely constrained matrix flow occurs. The thermal residual stress field in the composite plays an insignificant role in the analysis. In addition, the indentation response is not sensitive to the spatial distribution of particles in the numerical model.

Acknowledgments

The authors thank N. Chawla for many valuable discussions and his contribution to the experiment.

References

1. ASM Handbook, Vols. 1 (1990), 2 (1991) and 8 (2000), 10th edn. ASM International, Materials park, OH.
2. S. SURESH, A. MORTENSEN and A. NEEDLEMAN, "Fundamentals of Metal Matrix Composites" (Butterworth-Heinemann, Stoneham, MA, 1993).
3. M. TAYA and R. J. ARSENAULT, "Metal Matrix Composites-Thermomechanical Behavior" (Pergamon Press, Oxford, 1989).
4. N. CHAWLA and Y.-L. SHEN, *Adv. Engng. Mater.* **3** (2001) 357.
5. M. GUPTA, *High Temp. Mater. Processes* **17** (1998) 237.
6. Y.-L. SHEN, E. FISHENCORD and N. CHAWLA, *Scripta Mater.* **42** (2000) 427.
7. Y.-L. SHEN and N. CHAWLA, *Mater. Sci. Engng. A* **297** (2001) 44.
8. Y.-L. SHEN, J. J. WILLIAMS, G. PIOTROWSKI, N. CHAWLA and Y. L. GUO, *Acta Mater.* **49** (2001) 3219.
9. C. H. CACERES and W. J. POOLE, *Mater. Sci. Engng. A* **332** (2002) 311.
10. P. E. KRAJEWSKI, J. E. ALLISON and J. W. JONES, *Metall. Mater. Trans.* **24A** (1993) 2731.
11. N. CHAWLA, U. HABEL, Y.-L. SHEN, C. ANDRES, J. W. JONES and J. E. ALISON, *ibid.* **31A** (2000) 531.
12. ASTM Standard E 18-84, 1984.
13. Y.-L. SHEN, M. FINOT, A. NEEDLEMAN and S. SURESH, *Acta Metall. Mater.* **42** (1994) 77.
14. Y.-L. SHEN, M. FINOT, A. NEEDLEMAN and S. SURESH, *ibid.* **43** (1995) 1701.
15. T. WILKINS and Y.-L. SHEN, *Computational Mater. Sci.* **22** (2001) 291.
16. B. D. KOZOLA, Master's Thesis, University of New Mexico, 2001.
17. ABAQUS, Version 5.8, Hibbit, Karlson and Sorensen, Inc., Pawtucket, RI.
18. M. C. SHAW and G. J. DeSALVO, *Trans. ASME J. Engng. Industry* **92** (1970) 480.
19. Y.-L. SHEN and Y. L. GUO, *Modelling Simul. Mater. Sci. Engng.* **9** (2001) 391.

Received 23 May
and accepted 5 November 2002